International Journal of
Mathematical Modelling & Computations
Vol. 06, No. 03, Summer 2016, 233- 241

Numerical Analysis of the Casimir Effect Due to a Scalar Field

A. Ghaffari [a] and M. R. Tanhayi [b,*]

[a,b] *Department of Physics, Islamic Azad University, Central Tehran Branch, PO. Code 14168-94351, Iran.*

Abstract. In this paper, we study the Casimir effect of a scalar field with Dirichlet boundary condition in some certain topologies. By numerical analysis we show that Casimir energy is a shape-dependent quantity. We also obtain the phase transition in different topologies in which the Casimir force changes from attractive to repulsive or vice versa.

Received: 8 April 2016, Revised: 15 May 2016, Accepted: 5 June 2016.

Keywords: Casimir effect, Dirichlet boundary condition, Numerical analysis.

Index to information contained in this paper

1. Introduction

The Casimir effect, discovered more than 60 years ago in the seminal paper by Casimir (1948), it is one of the most direct manifestations of the existence of zero point vacuum oscillations. This effect is a manifestation of the non-trivial properties of the vacuum state in quantum field theory, and it is a macroscopic quantum effect. The Casimir effect, in its simplest form, is the attraction between two electrically neutral, infinitely large, parallel conducting planes placed in a vacuum. In fact, both parallel planes are mutually attracted to each other by the simple presence of the vacuum [1, 2]. For many years the Casimir effect was little more than a theoretical curiosity, but starting from the 1970's it has rapidly received increasing attention and in the last few years has become highly admired [2]. In the old days of classical mechanics the idea of a vacuum was simple. The vacuum was what remained if you emptied a container of all its particles and lowered the temperature down to absolute zero. The arrival of quantum mechanics, however, completely changed our

*Corresponding author. Email: m-tanhayi@iauctb.ac.ir

notion of a vacuum. All fields in particular electromagnetic fields have fluctuations. The vacuum is not really empty. It is filled with virtual particles, which are in a continuous state of fluctuation. Virtual particle-antiparticle pair can be created from vacuum and annihilated back to vacuum. These virtual particles exist for a time dictated by Heisenberg Uncertainty relation: $\Delta E \cdot \Delta t \approx \hbar$.
Photons (quanta of electromagnetic waves) are the dominant virtual particles in vacuum fluctuations but other particles produced as well. As a matter of fact vacuum is not simply nothing at all, but is best pictured as a superposition of many different states of electromagnetic field. Thus the creation and subsequent absorption of a photon by the vacuum implies vacuum fluctuates. In the ideal situation, at zero temperature for instance, there are no real photons between the plates. So it is only the vacuum, i.e., the ground state of quantum electrodynamics (QED) which causes the plates to attract each other. In other words at any given moment their actual value varies around a constant, mean value. Even a perfect vacuum at absolute zero has fluctuating fields known as *vacuum fluctuations*, the mean energy of which corresponds to half the energy of a photon. Remarkably the attractive force is independent of the coupling of electromagnetic (EM) field to matter (viz., the electronic charge) and is proportional to the velocity of light, c and Planck's constant, h.

As it is known the origin of the Casimir effect is essential geometrical and since the space between two plates is different from the space outside, the vacuum fluctuations are also different in the two regions. On the other hand fluctuations exert different forces on the plates from inside and outside, resulting in a net pressure, Casimir force and particle statistics. Particles other than photon also contribute a small effect but only the photon force is measurable. It is worth to mention that all bosons such as photons produce an attractive Casimir force while fermions make a repulsive contribution [1]. When one studies the Casimir effect, the zero point energy of the confined system should be calculated, and regularized. There are many methods of regularization such as *frequency cutoff regularization*, *Greens function method*, *zeta function regularization*, *dimensional regularization*, and *point-splitting method*, etc. The zero point energy after regularization is divergent, and thus it needs renormalization, which, briefly, aims at shifting the divergent part of the ground state energy from the ground state energy to the classical energy. Historically, it was Casimir who first subtracted from the infinite vacuum energy of the quantized electromagnetic field in the presence of ideal-metal planes the infinite vacuum energy of the same field in free Minkowski space. Both infinite energies were regularized, and after subtraction, the regularization was removed, leaving a finite energy per unit area, which depends on the separation distance a between the planes. This operation is applied to the operators of all physical observables, defined in free Minkowski space and written in a symmetrical form with respect to the creation and annihilation operators. Actually regularization is a method to change an infinite quantity into a finite one. A regularization parameter is introduced such that, in the appropriate limit, the original expression is restored. Of course, this procedure is not unique and beyond this formal definition, regularizations sometimes have a direct physical meaning. For instance, since ideal conductors do not exist in nature, one has in all real applications some natural frequency, usually of the order of the plasma frequency, beyond which the reflectivity rapidly decreases. However, this decrease might not provide a regularization for some systems. In a frequency cutoff regularization, one introduces some cutoff function in the mode expansion which makes the corresponding sum/integral converge. In a zeta function regularization, one temporarily changes the power of frequency in the mode sum energy [3–5, 7, 10]. We use numerical methods to compute the related equations (for example see the related computations of [6]).

The main aim of this paper is to compute the Casimir energy for different topologies and more interestingly we find the phase transition in which the Casimir force change its sign. To our knowledge this peculiar effect in our cases has not been reported. This paper is organized as follows: In section 2 we recall the Casimir energy in a rectangle. Section 3 is devoted to the calculation of the Casimir energy in 3 dimensional configurations. We show that within a specific choice of the free parameters of he theory the phase transition takes place. Finally the paper ends with a brief conclusion.

2. The Scalar Casimir Effect in a Rectangle

The Casimir energy and force may change sign depending on the geometry of the configuration and the type of boundary conditions. A dramatic example of this situation, which has given rise to many discussions in the literature for several decades, is the case of a rectangular box with sides a, b, and c. Lukosz (1971) noticed that the electromagnetic Casimir energy inside an ideal-metal box may change sign depending on side lengths a, b, and c. A detailed investigation of the Casimir energy for fields of different spins, where it may again be either positive or negative, inside a rectangular box as a function of the box dimensions was performed by Mamayev and Trunov (1979a, 1979b). In particular, analytical results for two- and three-dimensional boxes were obtained by repeated application of the AbelPlana formula. Ambjorn and Wolfram (1983) used the Epstein zeta function to calculate the Casimir energy for a scalar and an electromagnetic field in hypercuboidal regions in n-dimensional spacetime. The problem of isolation of the divergent terms in the vacuum energy and their interpretation received the most attention. In recent years, this problem has been reformulated in terms of a rectangular box divided into two sections by an ideal-metal movable partition (piston) (Cavalcanti 2004, Hertzberg et al. 2005). In this article for regularization of Epstein zeta function is used. In the beginning we must calculate the cavity modes. We start with a scalar field $\varphi(\vec{x},t)$ obeying the KleinGordon equation in four-dimensional spacetime

$$\left(\Box + \frac{m^2c^2}{\hbar^2}\right)\varphi(\vec{x},t) = 0. \tag{1}$$

Here m is the mass of the field and the four-dimensional d'Alembert operator is defined by

$$\Box \equiv \frac{1}{c^2}\frac{\partial^2}{\partial t^2} - \nabla^2. \tag{2}$$

Note that this scalar field in four-dimensional space-time is dimensionless. By applying the Dirichlet boundary condition on each of the walls,

$$\varphi(\vec{x}=0) = \varphi(x=a_1) = \varphi(y=a_2) = \varphi(z=a_3) = 0, \tag{3}$$

the solutions are obtained as

$$\varphi^{(\pm)}_{n\ell p}(\vec{x},t) = \mathbf{A}\, e^{\mp i\omega_{n\ell p}t}\sin(k_n\, x)\,\sin(k_\ell\, y)\,\sin(k_p\, z), \tag{4}$$

where

$$k_n = \frac{n\,\pi}{a_1}, \qquad k_\ell = \frac{\ell\,\pi}{a_2}, \qquad k_p = \frac{p\,\pi}{a_3}, \qquad n, \ell, p = 1, 2, 3, \ldots$$

$$\omega_{n\ell p} = \left[\frac{m^2 c^4}{\hbar^2} + c^2\,\left(k_n^2 + k_\ell^2 + k_p^2\right)\right]^{\frac{1}{2}}. \tag{5}$$

In this case, the scalar product of the two (in general complex) solutions of eqn (1), f and g, is

$$(f, g) = i\int_0^a \int_0^b \int_0^c dx^1\,dx^2\,dx^3 \left(f^* \frac{\partial g}{\partial x_0} - \frac{\partial f^*}{\partial x_0} g\right) \tag{6}$$

where $x_0 = x^0 = ct$. Therefore, the solutions of the Klein-Gordon equation can be written as follows

$$\varphi^{(\pm)}_{n\ell p}\,(\vec{x}, t) = \sqrt{\frac{4c}{a_1 a_2 a_3\,\omega_{n\ell p}}}\,e^{\mp i\omega_{n\ell p} t}\sin(k_n\,x)\,\sin(k_\ell\,y)\,\sin(k_p\,z). \tag{7}$$

The energy of the ground state in this case is as follows

$$\begin{aligned} E_0(a_1, a_2, a_3, m) &= \frac{\hbar}{2}\sum_{n,\ell,p=1}^{\infty} \qquad\qquad (8)\\ &= \frac{\hbar}{2}\sum_{n,\ell,p=1}^{\infty}\left\{\frac{m^2c^4}{\hbar^2} + c^2\pi^2\left[\left(\frac{n}{a_1}\right)^2 + \left(\frac{\ell}{a_2}\right)^2 + \left(\frac{p}{a_3}\right)^2\right]\right\}^{\frac{1}{2}} \end{aligned}$$

For a rectangular, one can show that

$$\varphi^{(\pm)}_{n\ell p}\,(t, x, y) = \sqrt{\frac{2}{ab\omega_{n\ell}}}\,e^{\mp i\omega_{n\ell} t}\sin(k_n\,x)\,\sin(k_\ell\,y) \tag{9}$$

in which the zero-point energy becomes

$$E_0(a, b) = \frac{\pi}{2}\sum_{n,\ell=1}^{\infty}\left[\left(\frac{n}{a}\right)^2 + \left(\frac{\ell}{b}\right)^2\right]^{\frac{1}{2}}, \tag{10}$$

where

$$k_n = \frac{n\,\pi}{a_1}, \qquad k_\ell = \frac{\ell\,\pi}{a_2}, \qquad \omega^2_{n,\ell} = k_n^2 + k_\ell^2, \qquad n, \ell = 1, 2, 3, \ldots. \tag{11}$$

Note that n and ℓ cannot be equal to zero because in that case the solution (10) vanishes. The Epstein zeta function and its analytic continuation are very convenient tools for the investigation of the analytic properties of multiple summations.

The Epstein zeta function can be defined as (Erd‘elyi et al. 1981)

$$Z_p\left(\frac{1}{a_1},\frac{1}{a_2},\dots,\frac{1}{a_p};s\right)=\sum_{n_1,\dots,n_p=-\infty}^{\infty}\left[\left(\frac{n_1}{a_1}\right)^2+\dots+\left(\frac{n_p}{a_p}\right)^2\right]^{-s/2}\left(1-\delta_{n_1}\cdots\delta_{n_p}\right). \tag{12}$$

Note that the inclusion of the negative product of δ-symbols is equivalent to the condition that the term with all $n_i = 0$ is omitted. The series in eqn (12) is convergent when $Re[s] > p$. Equation (10) can be expressed in terms of the Epstein and Riemann zeta functions in the following way:

$$E_0^{(s)}(a,b)=\frac{\pi}{8}\left\{Z_2\left(\frac{1}{a},\frac{1}{b};s-1\right)+2\left(\frac{1}{a}+\frac{1}{b}\right)\zeta_R(s-1)\right\}, \tag{13}$$

In the limiting case $s \to 0$ (i.e. when the regularization is removed), the quantity (13) is divergent. By using the reflection relations for the Riemann zeta function and for the Epstein zeta function as follows,

$$\begin{cases}a_1\cdots a_p\,\Gamma(\frac{s}{2})\,\pi^{-s/2}\,Z_p(a_1,a_2,\dots,a_p;s)=\Gamma(\frac{p-s}{2})\,\pi^{(s-p)/2}\,Z_p\left(\frac{1}{a_1},\frac{1}{a_2},\dots,\frac{1}{a_p};p-s\right)\\ \Gamma(\frac{s}{2})\,\zeta_R(s)=\pi^{(2s-1)/2}\,\Gamma(\frac{1-s}{2})\,\zeta_R(1-s)\end{cases} \tag{14}$$

we finally obtain the finite Casimir energy for a rectangle (After removing the regularization),

$$E_0(a,b)=-\frac{ab}{32\pi}Z_2(a,b;3)+\frac{\pi}{48}\left(\frac{1}{a}+\frac{1}{b}\right). \tag{15}$$

where Z_2 is defined by

$$\begin{aligned}Z_2(a,b;3)&=\frac{2\pi^{\frac{3}{2}}}{\Gamma\left(\frac{3}{2}\right)}\sum_{\ell=1}^{\infty}S\left(\pi b\ell,\frac{1}{a};3\right)+2\frac{\zeta_R(3)}{a^3}\\&=\frac{2\pi^2}{32ab^2}+\frac{16\pi}{a^2b}\sum_{n,\ell=1}^{\infty}K_1\left(2\pi n\ell\frac{b}{a}\right)+2\frac{\zeta_R(3)}{a^3}\\&=\frac{2\pi^2}{32ab^2}+2\frac{\zeta_R(3)}{a^3}-\frac{32\pi^2}{a^2b}G\left(\frac{b}{a}\right)\end{aligned} \tag{16}$$

in which

$$\begin{aligned}G(z)&\equiv -z\int_1^{\infty}du\,\sqrt{u^2-1}\sum_{n=1}^{\infty}\frac{n^2}{e^{-2\pi n\ell uz}-1}\\&=-\frac{1}{2\pi}\sum_{n=1}^{\infty}\sum_{\ell=1}^{\infty}\frac{n}{\ell}K_1(2\pi n\ell z).\end{aligned} \tag{17}$$

$$\begin{aligned}S(\eta,\kappa,q)&\equiv\pi^{-q/2}\,\Gamma\left(\frac{q}{2}\right)\sum_{k=1}^{\infty}\left[\left(\frac{\eta}{\pi}\right)^2+\left(\frac{k}{\kappa}\right)^2\right]^{-q/2}\\&=\kappa\left(\frac{\eta}{\sqrt{\pi}}\right)^{1-q}\left[\Gamma\left(\frac{q-1}{2}\right)+4\sum_{n=1}^{\infty}(\eta\kappa n)^{\frac{(q-1)}{2}}K_{\frac{(q-1)}{2}}(2\eta\kappa n)\right].\end{aligned} \tag{18}$$

Where $S(\eta, \kappa, q)$ is auxiliary function. The substitution of eqn (16) into eqn (15) the Casimir energy is found to be

$$E(a,b) = \frac{\pi}{48a} - \frac{b}{16\pi a^2}\zeta_R(3) + \frac{\pi}{a}G\left(\frac{b}{a}\right). \tag{19}$$

And consequently the Casimir force becomes:

$$F_a(a,b) = -\frac{\partial E(a,b)}{\partial a} = \frac{\pi}{48a^2} - \frac{b}{8\pi a^3}\zeta_R(3) + \frac{\pi}{a^2}G\left(\frac{b}{a}\right) + \frac{\pi b}{a^3}G^{'}\left(\frac{b}{a}\right) \tag{20}$$

$$F_b(a,b) = -\frac{\partial E(a,b)}{\partial b} = \frac{1}{16\pi a^2}\zeta_R(3) - \frac{\pi}{a^2}G^{'}\left(\frac{b}{a}\right). \tag{21}$$

The important fact is that this energy is symmetric with respect to the interchange of a and b. This symmetry is, however, implicit. Numerical computations using the full equation (19) show that the Casimir energy E is positive if

$$0.34278 < \frac{b}{a} < 2.73687.$$

The 3D plot of the casimir energy for a rectangle and its contour plot is showed in figure (1).

3. A Massless Scalar Field in a 2-Torus

In the previous sections, we have considered Dirichlet boundary conditions imposed on scalar field of rectangle. Similar results can be obtained for different types of boundary conditions. As a simple case, let us begin with a massless scalar field in a rectangle whose opposite sides are identified with each other (we have the topology of a 2-torus, which can be symbolically written as $S^1 \times S^1$). In this case In this case $k_n = \frac{2\pi n}{a}$ and $\kappa_\ell = \frac{2\pi \ell}{b}$, the vacuum energy is given by

$$E_0(a,b) = \pi \sum_{n,\ell=-\infty}^{\infty} \left[\left(\frac{n}{a}\right)^2 + \left(\frac{\ell}{b}\right)^2\right]^{\frac{1}{2}} \tag{22}$$

Noting that the term with $n = \ell = 0$ does not contribute to the Casimir energy, one can write

$$E_0^{(s)}(a,b) = \pi \sum_{n,\ell=-\infty}^{\infty} (1 - \delta_{n_0}\delta_{\ell_0}) \left[\left(\frac{n}{a}\right)^2 + \left(\frac{\ell}{b}\right)^2\right]^{-\frac{(s-1)}{2}} = \pi Z_2\left(\frac{1}{a}, \frac{1}{b}; s-1\right) \tag{23}$$

After regularization and making use of the Z_2, one obtains

$$E(a,b) = -\frac{\pi}{24b} - \frac{\zeta_R(3)b}{2\pi a^2} + \frac{4\pi}{a}G\left(\frac{2b}{a}\right) + \frac{\pi}{12a} \tag{24}$$

The 3D plot of the casimir energy for a 2-torus and its contour plot is showed in figure (2).

4. A Massless Scalar Field in a Hybrid

It is of some interest to consider a hybrid situation, for example an identification condition on one pair of sides of a rectangle, and a Dirichlet boundary condition on the other (we have the topology of $S^1 \times I$, where I is a Euclidean interval). The vacuum energy of a massless scalar field takes the form

$$\begin{aligned} E_0(a,b) &= \pi \sum_{n=-\infty}^{\infty} \sum_{\ell=1}^{\infty} \left[\left(\frac{n}{a}\right)^2 + \left(\frac{\ell}{2b}\right)^2 \right]^{\frac{1}{2}} \\ &= \frac{\pi}{2} \sum_{n=-\infty}^{\infty} \sum_{\ell=-\infty}^{\infty} (1-\delta_{\ell_0}) \left[\left(\frac{n}{a}\right)^2 + \left(\frac{\ell}{2b}\right)^2 \right]^{\frac{1}{2}} \\ &= \frac{\pi}{2} \sum_{n,\ell=-\infty}^{\infty} (1-\delta_{n_0}\delta_{\ell_0}) \left[\left(\frac{n}{a}\right)^2 + \left(\frac{\ell}{2b}\right)^2 \right]^{\frac{1}{2}} - \frac{\pi}{a} \sum_{n=1}^{\infty} n \end{aligned} \tag{25}$$

Then the regularized vacuum energy in the hybrid configuration is

$$E_0^{(s)}(a,b) = \frac{\pi}{2} \left[Z_2\left(\frac{1}{a}, \frac{1}{2b}; s-1\right) - \frac{2}{a}\zeta_R(s-1) \right] \tag{26}$$

After application of the reflection relation (14), the following finite result is obtained

$$E(a,b) = -\frac{ab}{4\pi} Z_2(a, 2b, ; 3) + \frac{\pi}{12a} \tag{27}$$

which can be written as

$$E(a,b) = -\frac{\pi}{24b} - \frac{\zeta_R(3)b}{2\pi a^2} + \frac{4\pi}{a} G\left(\frac{2b}{a}\right) + \frac{\pi}{12a} \tag{28}$$

The 3D plot of the casimir energy for a hybrid and its contour plot is showed in figure (3). As a result, we collect the Casimir energy range for a scalar field with different topologies in table.(1).

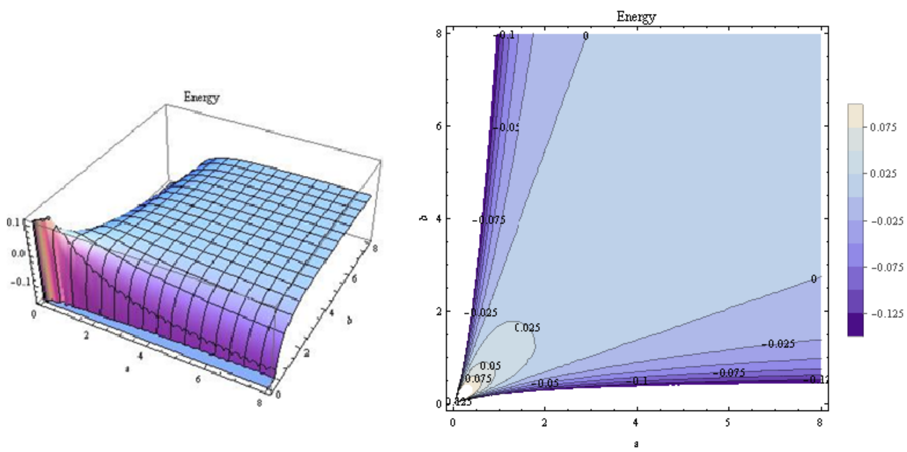

Figure 1. Left: The Casimir energy for a scalar field in a rectangular, Right: The contour plot of the Casimir energy

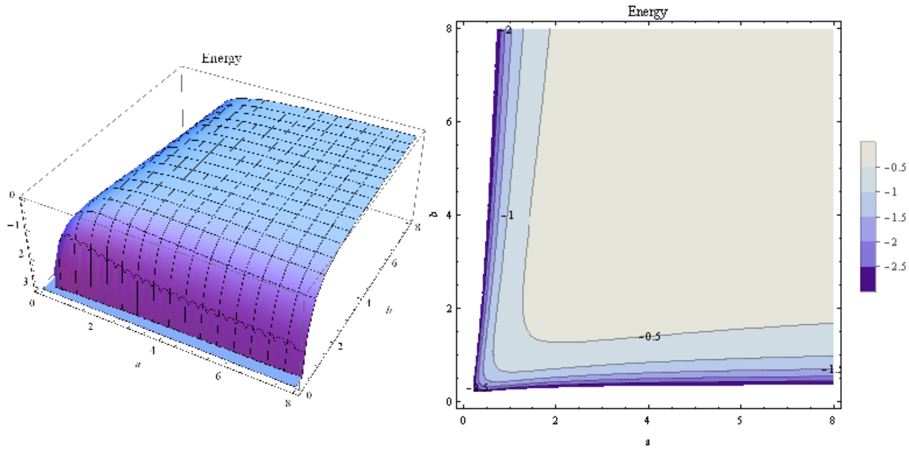

Figure 2. Left: The Casimir energy for a scalar field in a 2-torus, Right: The contour plot of the Casimir energy

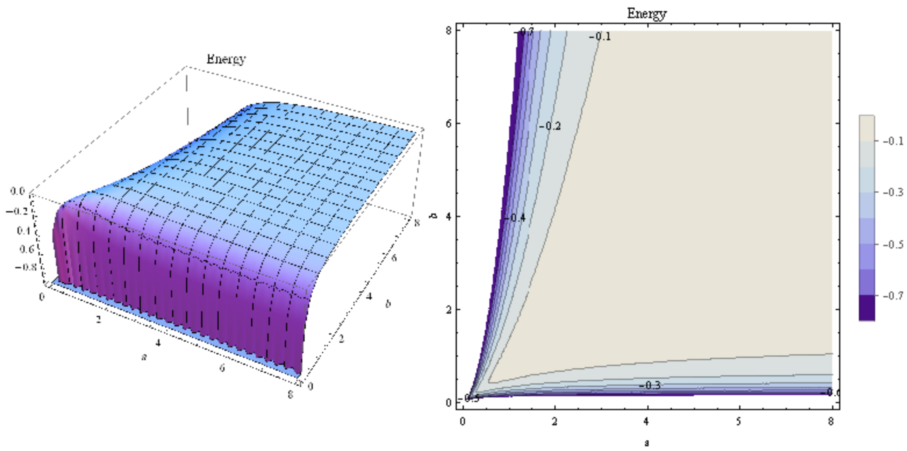

Figure 3. Left: The Casimir energy for a scalar field in a hybrid, Right: The contour plot of the Casimir energy

		Rectangle	2-torus	Hybrid
Energy	Possitive energy	$0.34278 \le \frac{b}{a} \le 2.73687$	—	—
	Negative energy	$\frac{b}{a} > 2.73687$, $\frac{b}{a} < 0.34278$	Consistently Negative	Consistently Negative
Force on plane a	Possitive force	$0 \le \frac{b}{a} \le 1.37513$	$0 \le \frac{b}{a} \le 0.592595$	$0 \le \frac{b}{a} \le 0.684434$
	Negative force	$\frac{b}{a} > 1.37513$	$\frac{b}{a} > 0.592595$	$\frac{b}{a} > 0.684434$
Force on plane b	Possitive force	$\frac{b}{a} \ge 0.722587$	$\frac{b}{a} \ge 1.65574$	$\frac{b}{a} \ge 0.827218$
	Negative force	$\frac{b}{a} < 0.722587$	$\frac{b}{a} < 1.65574$	$\frac{b}{a} < 0.827218$

Table(1): The Casimir energy range for a scalar field with different topologies

5. Conclusion

An attractive force between two uncharged parallel conducting plates, which is known as Casimir force, showed that finite differences between different configurations of infinite energy have physical interpretation. The advent of divergence in expectation value of the energy-momentum tensor and consequently in zero-point energy leads to fundamental problems in modern physics. In non-gravitational

physics, regarding this fact that only changes in energy from one state to another are measurable, any resulted infinite vacuum energy in QFT may be renormalized -or rescaled- by subtracting infinite energy from quantum vacuum energy.
There are few instances wherein the Casimir effect can give rise to repulsive forces between uncharged objects. Theoretically, one can explain the repulsive forces, in fact, this has sparked interest in applications of the Casimir effect toward the development of levitating devices. However, such a repulsive force has been detected recently [9]. Casimir repulsion can in fact occur for sufficiently anisotropic electrical bodies [8]. By numerical analysis, in this study we study the phase transition of the Casimir energy. Our results show that not only the Casimir energy depends on a topology, but ia a given topology by changing the parameters one my receive a phase transition of repulsive and attractive Casimir force.

Acknowledgments

The authors would like to thank M. Amraji for his corporation and interest in this work. This work has been supported partially by Islamic Azad University Central Tehran Branch.

References

[1] Bordag, M., Klimchitskaya, G. L., Mohideen, U and Mostepanenko, V. M. Advances in the Casimir Effect. Oxford University Press Inc, (2009).
[2] Bordag, M., Mohideen, U and Mostepanenko, V. M. New Developments in the Casimir Effect. A. A. Maradudin (ed). Physics Reports, **353** (2001) 1205.
[3] Edery. Ariel, Multidimensional Cut-Off Technique, Odd-Dimensional Epstein Zeta Functions and Casimir Energy of Massless Scalar Fields, Journal of Physics A: Mathematical and Theoretical, **39 (3)** (2006) 685-712.
[4] Elizalde. E, Odintsov. S. D, Romeo. A and Andrei. A, Zeta Regularization Techniques with Applications, World Scientific Publishing Co. Pte. Ltd.
[5] Elizalde. E, Ten Physical Applications of Spectral Zeta Functions, Springer, (1995).
[6] Khayyari. O. El and Lamnii. A, Numerical Solutions of Second Order Boundary Value Problem by Using Hyperbolic Uniform B-Splines of Order 4, International Journal of Mathematical Modelling and Computations, **4 (1)** (2014).
[7] Kirsten. K and Williams. F. L. (ed), A Window into Zeta and Modular Physics. Cambridge University Press, (2010).
[8] Milton. K. A, Abalo. E. K, Parashar. Prachi, Pourtolami. Nima, Brevik. Iver and Ellingsen. Simen. A "Repulsive Casimir and Casimir-Polder Forces". J. Phys. A : 4006. arXiv:1202.6415v2, **45 (37)** (2012).
[9] Munday. J. N, Capasso. F and Parsegian. V. A, "Measured long-range repulsive Casimir-Lifshitz forces, **457** (2009) 3-170.
[10] Ruggiero. J. R., Zimerman. A. H and Villani. A, Application of Analytic Regularization to the Casimir Forces. Revista Brasileira de Fsica, **7 (3)** (1977).